Electronic Supplementary Material (ESI) for Journal of Materials Chemistry A.

Supporting information

Hierarchical heterostructures of Sn_3O_4 on N doped TiO_2 nanotubes with enhanced photocatalytic performances

Xin Yu[ab1], Longfei Wang[ab1], Jian Zhang[ab], Weibo Guo[ab], Zhenhuan Zhao[c], Yong Qin[a], Xiaoning Mou[a], Aixue Li[a]*, Hong Liu[ac]*

[a]Beijing Institute of Nanoenergy and Nanosystems, Chinese Academy of Science, Beijing 100083, China

[b]University of Chinese Academy of Science, Beijing 100049, China

[c]State Key Laboratory of Crystal Materials, Shandong University, Jinan 250100, China

*Corresponding author. E-mail addresses: hliu@binn.cas.cn (H. Liu), liaixue@binn.cas.cn (A. Li)

Xin Yu and Longfei Wang are contributed equally to this work.

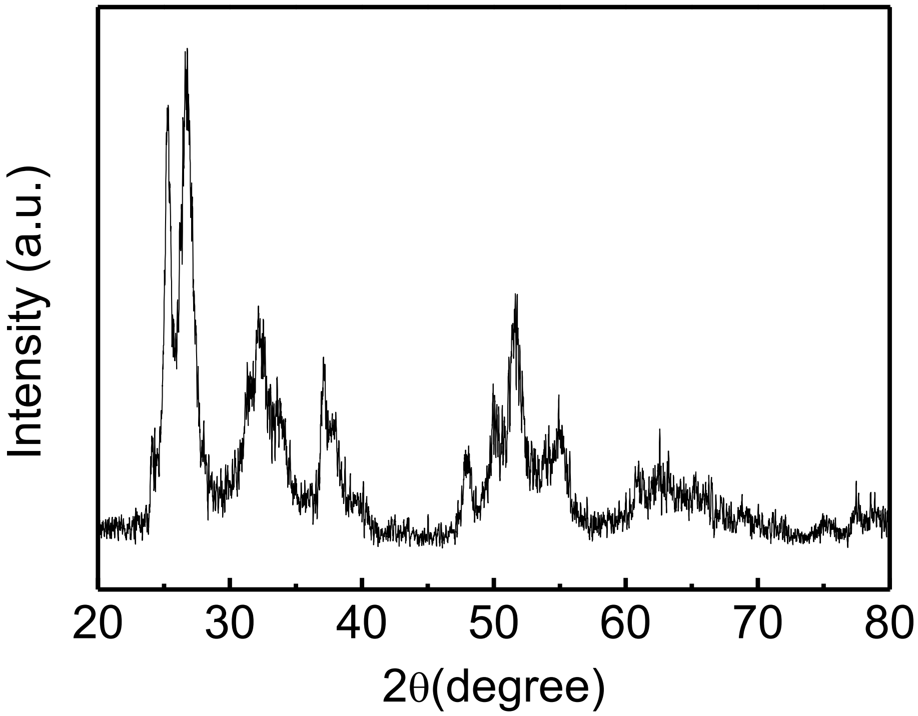

Fig. S1 XRD patterns of Sn_3O_4/TiO_2 heterostructures。

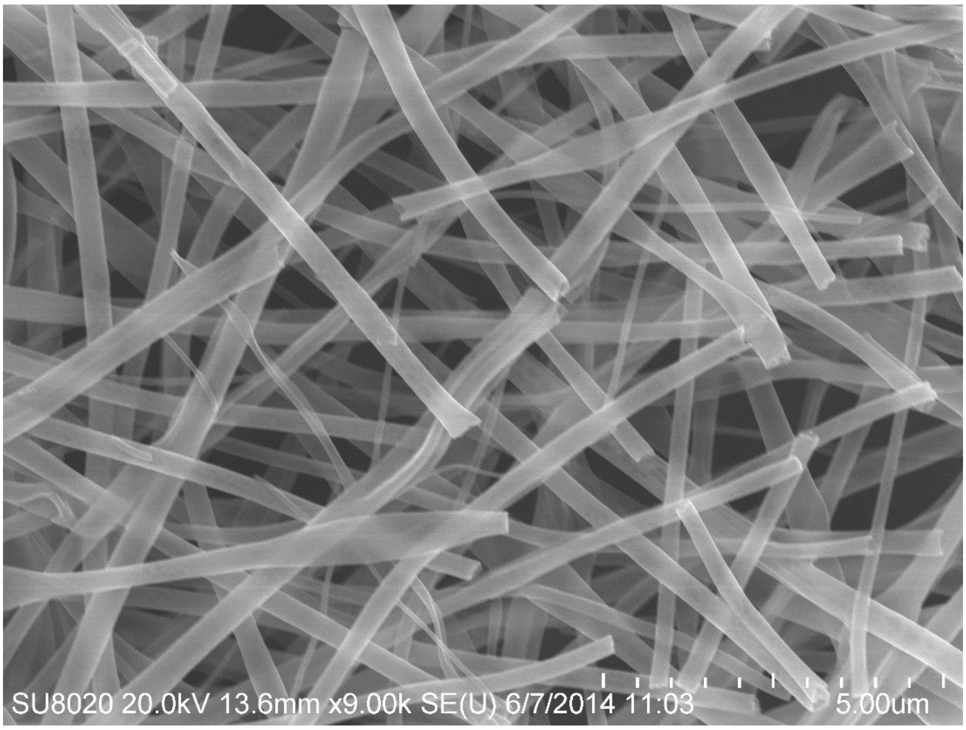

Fig. S2 SEM image of theTiO$_2$ nanotubes.

Sample number $N\text{-}TiO_2 : Sn_3O_4$	$N\text{-}TiO_2$	$SnCl_2 \cdot 2H_2O$	$Na_3C_6H_5C_3$
1:1	0.016 g	0.27 g	0.882 g
2:1	0.032 g	0.27 g	0.882 g
3:1	0.048 g	0.27 g	0.882 g
4:1	0.064 g	0.27 g	0.882 g

Table. S1 The detailed experimental conditions for the fabrication of molar ratio of $N\text{-}TiO_2$: Sn_3O_4 = 1:1, 2:1, 3:1 and 4:1

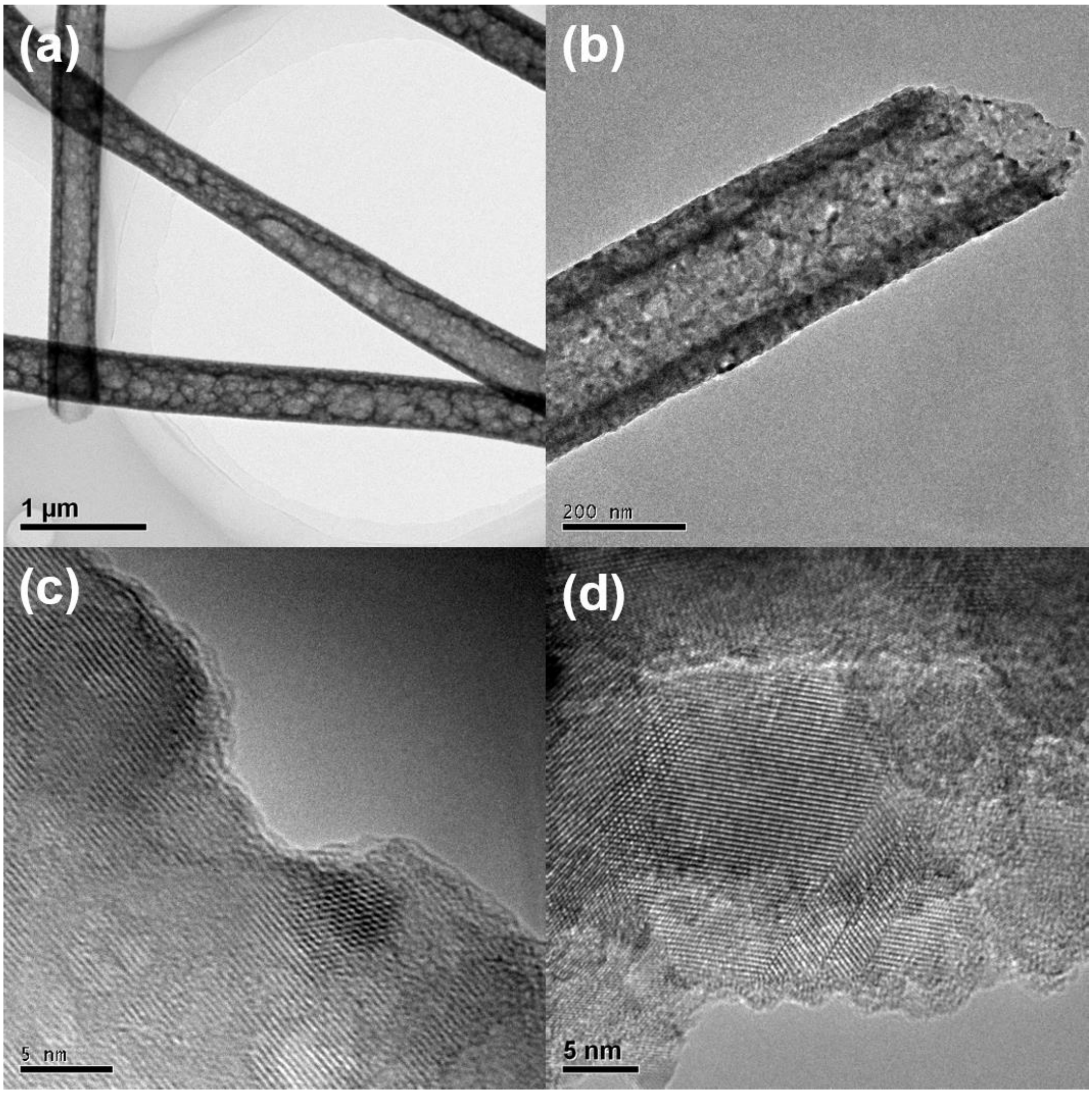

Fig. S3 TEM image of the (a, b) N-TiO_2 nanotubes, (c, d) HRTEM of the N-TiO_2 nanotubes.

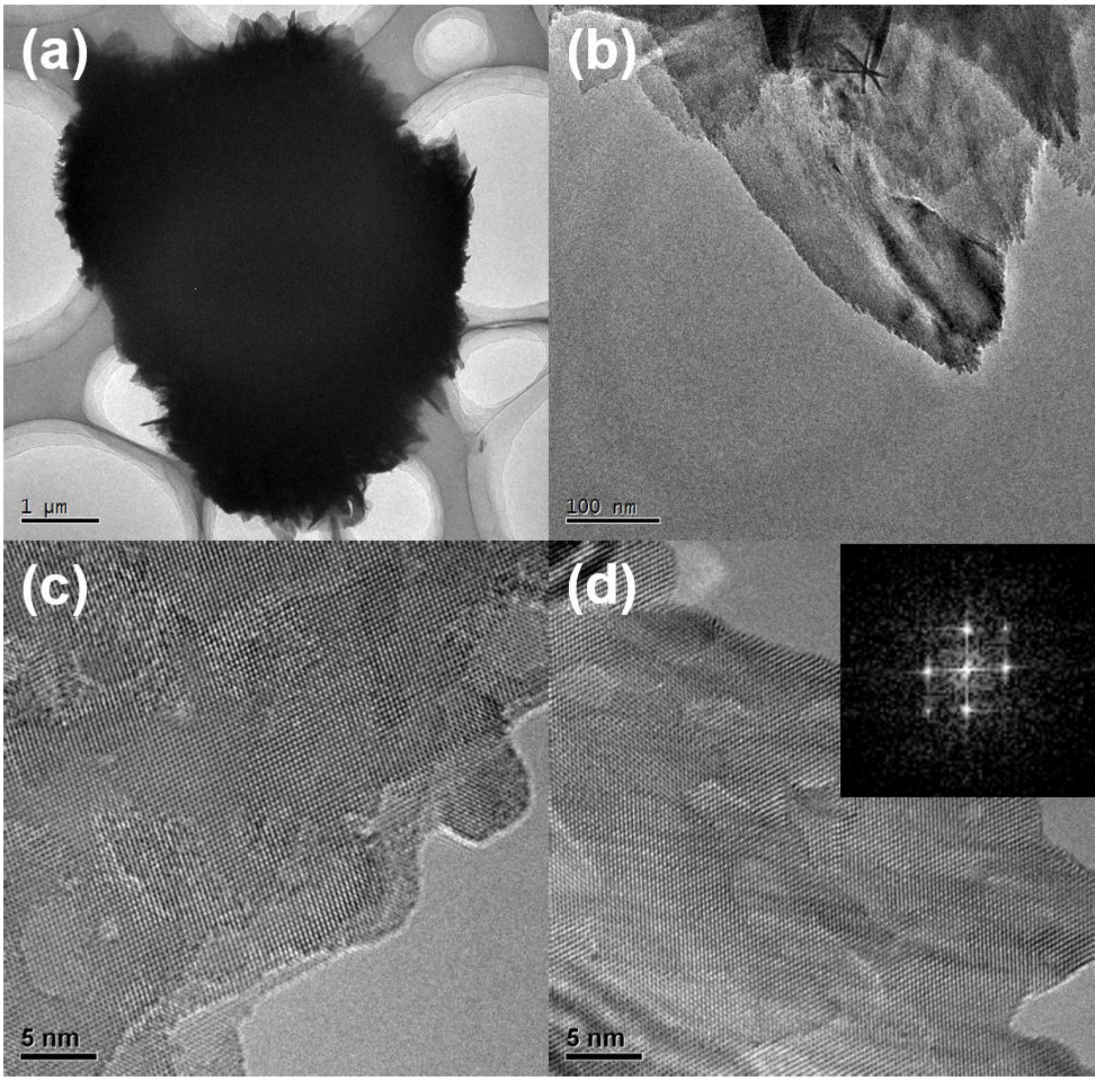

Fig. S4 (a, b) TEM images of the Sn_3O_4 nanosheets, (c, d) HRTEM images of the Sn_3O_4 nanosheets.

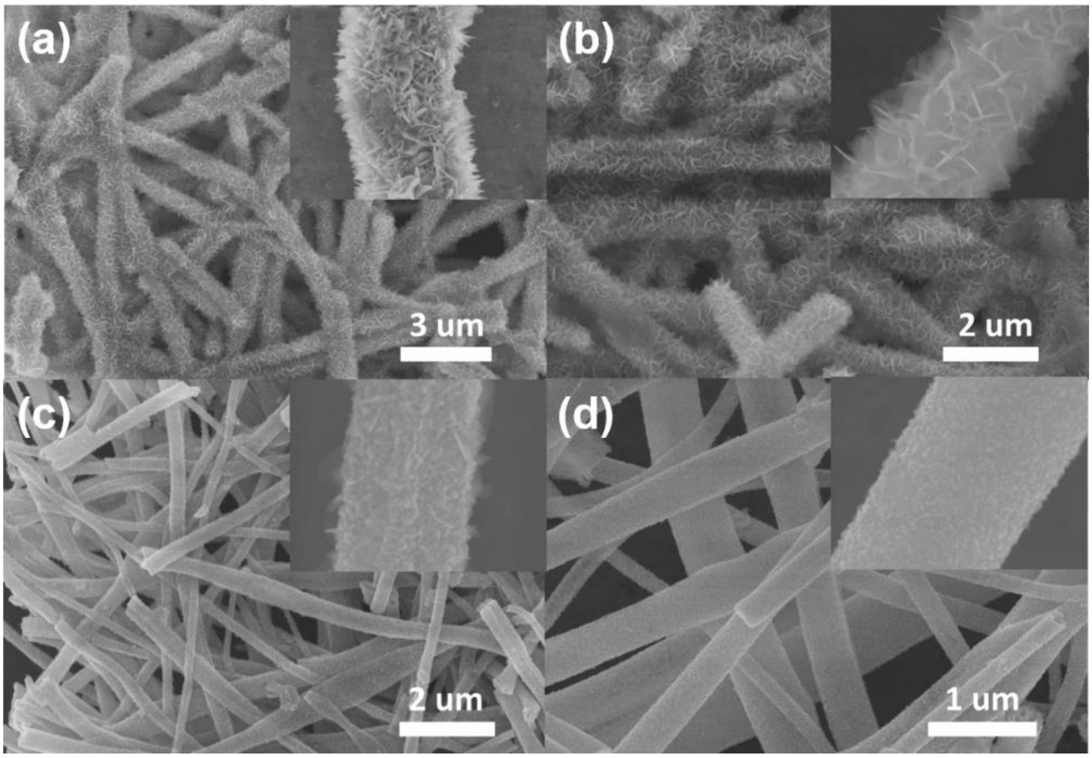

Fig. S5 SEM images Sn_3O_4/N-TiO_2 hierarchical heterostructures on different molar ratio (a) N-TiO_2: Sn_3O_4 = 1:1 (b) N-TiO_2: Sn_3O_4 = 2:1 (c) N-TiO_2 : Sn_3O_4 = 3:1 (d) N-TiO_2 : Sn_3O_4 = 4:1

The morphology of the samples was observed by FESEM. As observed in Fig. S5, four kinds of Sn_3O_4 nanostructures grew on the surface of TiO_2 nanotubes after solvothermal reaction for 12 h. Fig. 5 show the SEM images of samples, respectively. From Fig. 5d, it was found that a number of Sn_3O_4 nanoparticles uniformly grew on the surface of TiO_2 nanotubes. And nanoparticles possess an average diameter of less than 50 nm. When the concentration of precursor Sn_3O_4 was increased 2 times, the morphology of Sn_3O_4 nanostructures grew on TiO_2 nanotubes changed significantly. As shown in Fig. 5c, several Sn_3O_4 nanosheets instead of nanoparticles grew on the surface of TiO_2 nanotubes and the nanosheets distribute uniformly. From the high magnification SEM image (inset of Fig. 5c), it could be seen that the Sn_3O_4 nanosheets were about 10 nm in thickness and 40–60 nm in length. In Fig. 5a and b, when the Sn_3O_4 concentration was further increased, Sn_3O_4 nanosheets instead of nanoparticles grew on the surface of TiO_2 and the density of the nanoparticles was dramatically increased compared with sample Fig. 5d. Notably, the nanoparticles were still uniformly distributed over each fiber without aggregation, although their density increased significantly. This might be due to the fact that the high porosity and large surface area of TiO_2 nanotubes were beneficial for the growth and uniform distribution of secondary nanostructure nanomaterials.

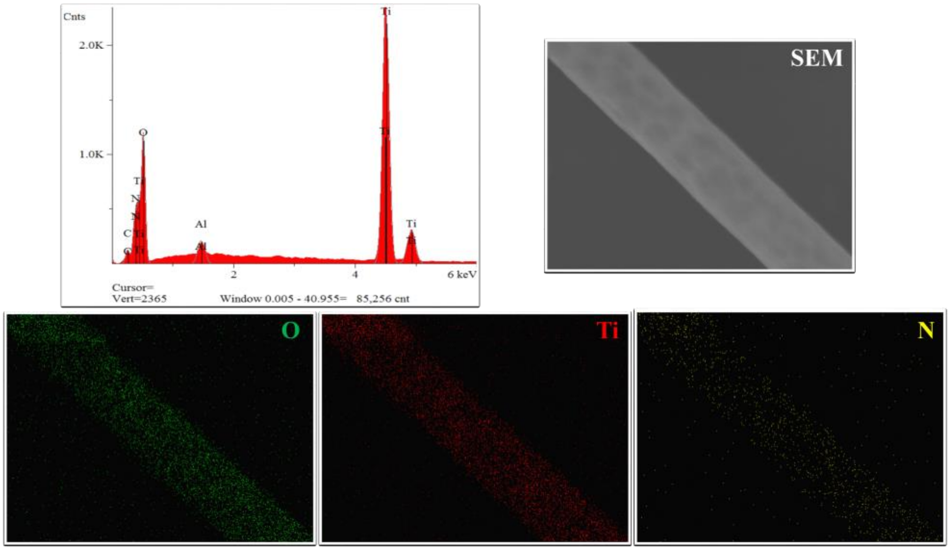

Fig. S6 EDS spectrum and mapping results from a single N-TiO_2 nanotube.

In addition, the energy dispersive X-ray spectrometry (EDS) analysis was conducted to confirm the composition of N-TiO_2. The elements, Al and C (from the SEM sample holder), N, O and Ti were all detected. The EDS mapping clearly shows the strongest signals of N, Ti, and O， , confirming that the N element was distributed uniformly.

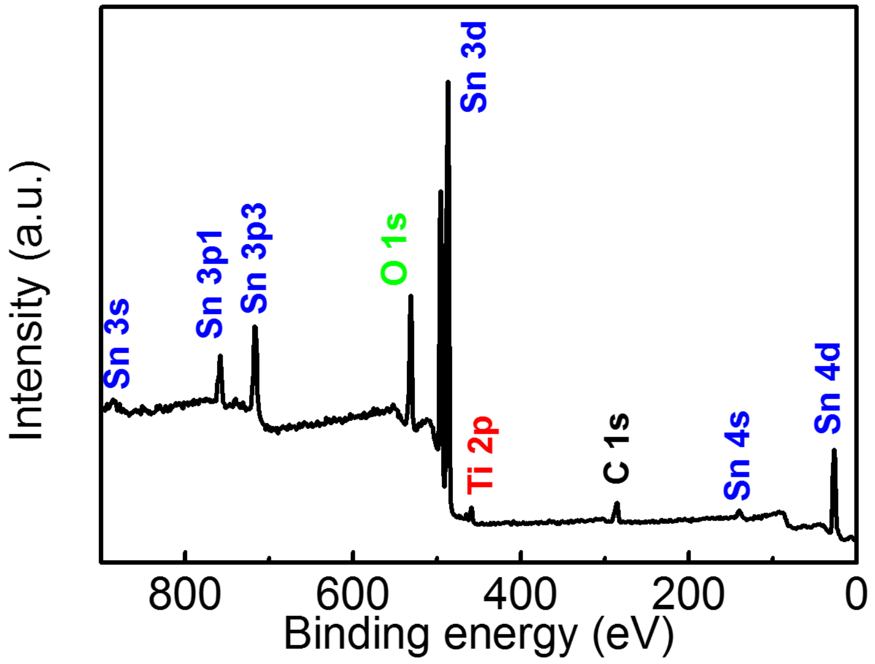

Fig. S7 XPS fully scanned spectrum of the Sn_3O_4/N-TiO_2 hierarchical heterostructures.

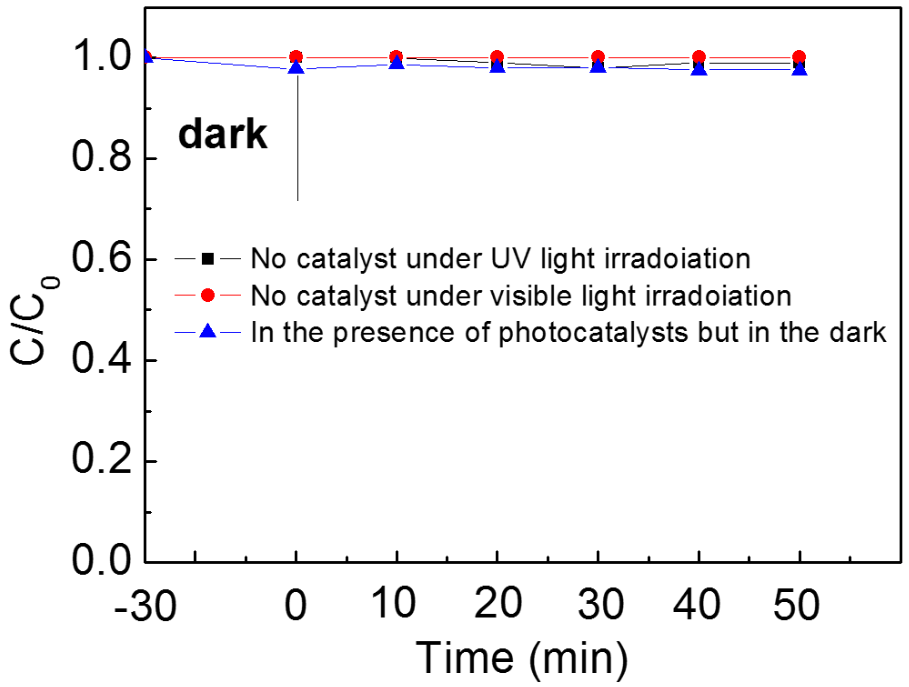

Fig. S8 Photocatalytic degradation of MO without any catalyst and in the presence of photocatalysts but in dark.

To check if MO can be degraded under light irradiation, 20 mg/L of MO solution without photocatalyst was irradiated under UV and visible light, respectively, and the degradation rate of MO were checked. The result shows that there is no decrease of MO without photocatalyst under UV and visible light irradiation. And these results indicated that the adsorption-desorption equilibrium of MO was established within 30 min in the dark. And there was no appreciable degradation of MO after 50 min in the absence of photocatalysts.

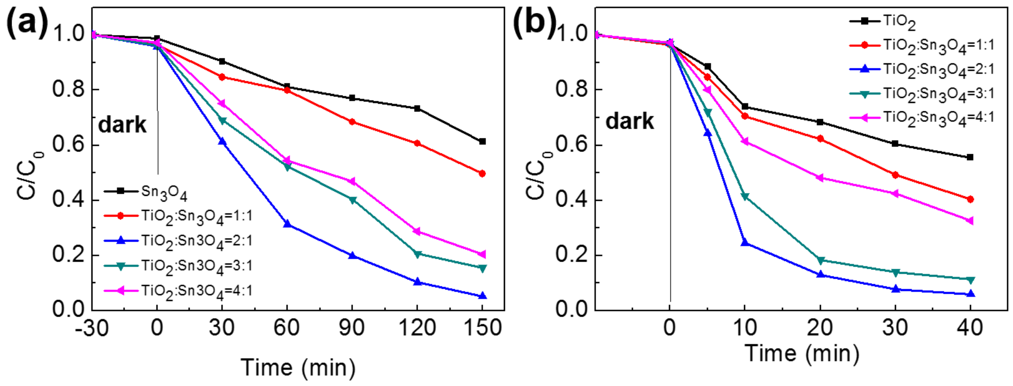

Fig. S9 comparison of the photocatalytic activities of the Sn_3O_4/TiO_2 hierarchical heterostructures at different mole ratios of TiO_2 and Sn_3O_4 under either (a) visible or (b) UV light irradiation.

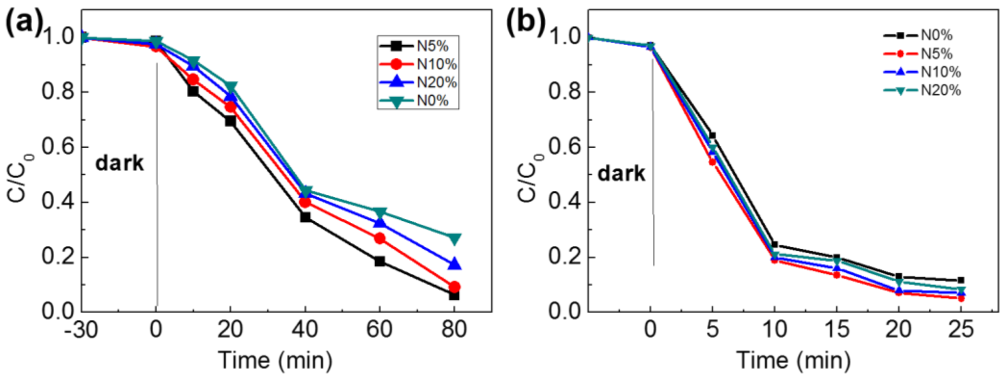

Fig. S10 Comparison of photocatalytic activities of the Sn_3O_4/N-TiO_2 hierarchical heterostructures (molar ratio N-TiO_2: Sn_3O_4 = 1:1) at different content of N under either (a) visible or (b) UV light irradiation.

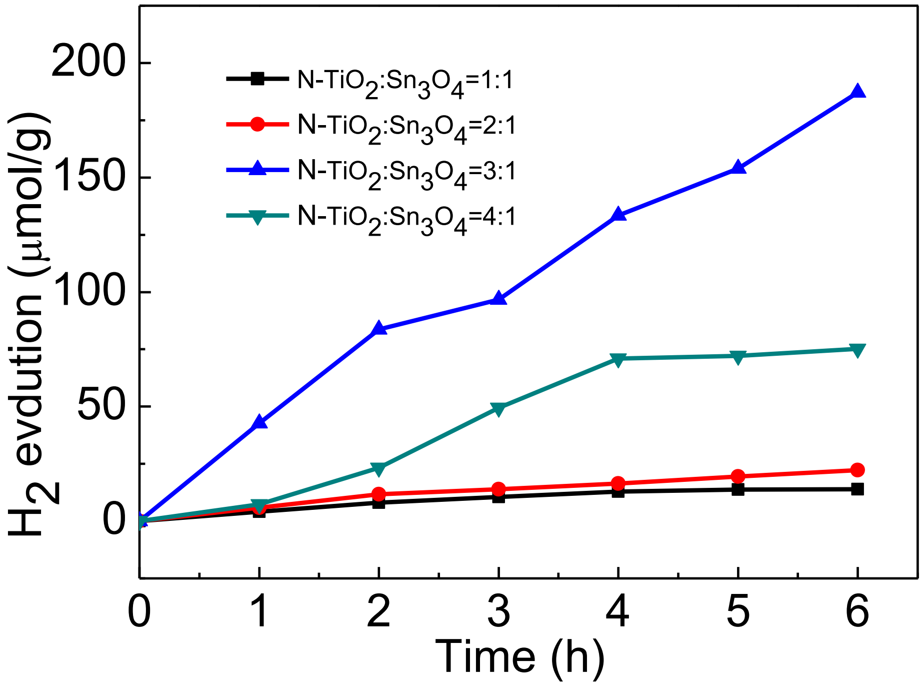

Fig. S11 Photocatalytic H_2 evolution from the aqueous methanol solution by Sn_3O_4/N (5%)-TiO_2 hierarchical heterostructure at different ratio of Sn_3O_4 and N (5%)-TiO_2.

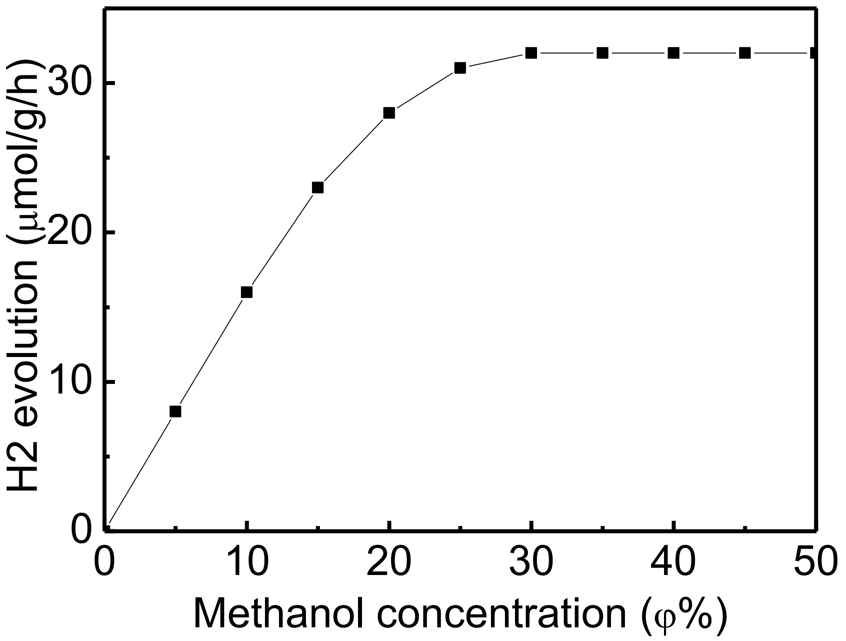

Fig. S12 The amount of produced H2 and the concentration of used methanol.

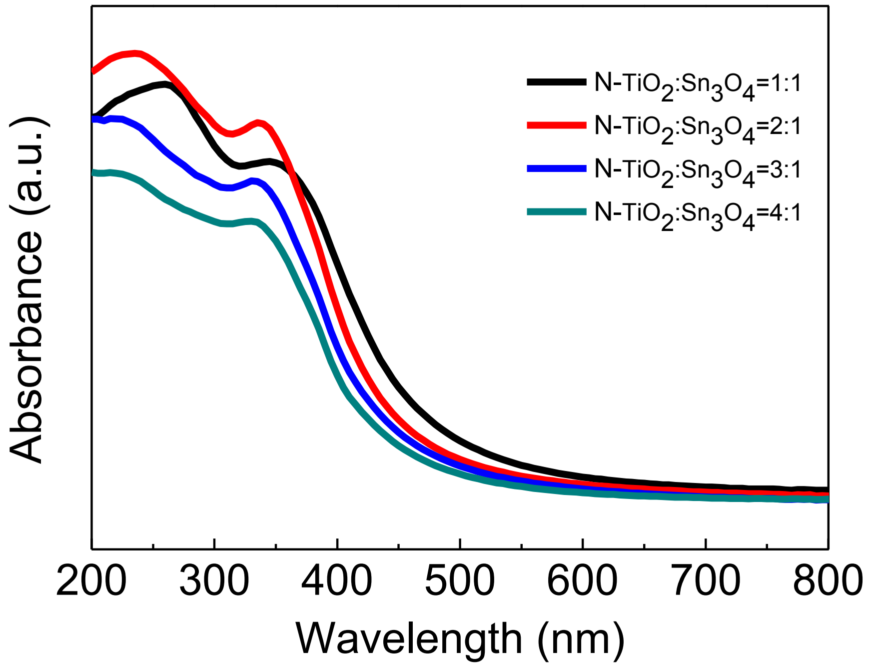

Fig. S13 UV-Vis diffuse reflectance spectra of Sn_3O_4/N (5%)-TiO_2 hierarchical heterostructures at different ratio of Sn_3O_4 and N-TiO_2.

The optical band gap of the as-prepared Sn_3O_4 was calculated using the Tauc model. By plotting $(\alpha h\nu)^2$ versus hv and extrapolating the linear portion of the spectrum in the band edge region, the optical band gap of the Sn_3O_4 microflowers was determined to be 2.95 ev.

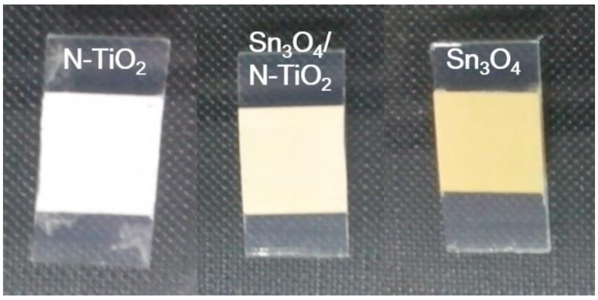

Fig. S14 Digital pictures of the N-TiO_2, Sn_3O_4/N-TiO_2 and Sn_3O_4 anode.